

### ***Additional File 1 – Supplemental Figures and Legends***

**Figure S1.** Run time comparison of scSNV, STAR Solo and Cell Ranger across 22 dscRNA-seq samples colored by the sample series. The runtime for scSNV (circle), Cell Ranger (triangle), and STAR Solo (square) in minutes versus the total number of reads in millions. The black lines indicate the ordinary least squares regression fit for scSNV (solid), Cell Ranger (dashed), and STAR Solo (dotted). For scSNV:  $R^2 = 0.466$ ,  $-\log_{10}(P) = 3.336$ , Cell Ranger:  $R^2 = 0.233$  -  $\log_{10}(P) = 1.638$ , and STAR Solo  $R^2 = 0.033$ ,  $-\log_{10}(P) = 0.381$ .

**Figure S2.** Comparison of spliced (**A, B, C**) and unspliced (**D, E, F**) counts from scSNV and Cell Ranger / Velocity. For each plot we are comparing the same set of barcodes extracted from scSNV and Cell Ranger (CR) using the quality barcodes identified by scSNV. (**A, D**) the total number of spliced and unspliced molecules for each barcode for scSNV (y-axis) and Cell Ranger (x-axis). The black diagonal line shows where values would be equal. (**B, E**) For each barcode pair from scSNV and Cell Ranger we calculated the spearman correlation between the spliced and unspliced counts between scSNV and Cell Ranger / Velocity. (**B, E**) boxplots of the spliced and unspliced counts for each sample. The x-axis includes the same name and number of cells compared. (**C, F**) the Spearman correlation for all samples vs the total molecules identified by scSNV for each barcode. Samples are colored by their tissue type as per the legend.

**Figure S3.** Collapsed read lengths for molecules with (**A**) two reads, (**B**) three reads, (**C**) four reads, and (**D**) five or more reads. Samples are ordered by their sequencing saturation (lowest to highest). For each sample the length distribution of the number of collapsed bases for each read was down-sampled to 20,000 reads, smoothed using gaussian kernel density estimation, and then scaled so the minimum and maximum value ranged from 0 to 1. The density values are indicated by the color bar. The sequencing saturation and PCR duplicate rate are indicated by the 2<sup>nd</sup> and

third color bars while the tissue type for each sample is indicated by the top color as per the legends.

**Figure S4.** SNV calling accuracy using matched whole genome data to estimate F1-scores (top), TPRs (middle) and FDRs (bottom) on the y-axis stratified by increasing minor allele fraction cut-offs (x-axis) for four alignment methods as indicated by the line color and three SNV calling tools as indicated above each graph. The median line for each tool and method is indicated with a solid line, samples with matched exome data are indicated with a dotted line and samples with WGS data are indicated with a dashed line.

**Figure S5.** Determining a minor allele fraction cutoff that maximizes the TPR and minimizes the FDR for SNVs called using scSNV Pileup. The TPR is on the x-axis and FDR on the y-axis and the lines are from applying increasingly stringent allele fraction cut-offs from 0.01 to 1.00. Each of the eleven samples with matched WGS data are shown individually as indicated above the plot, the color of each line indicates the alignment tool and the dot indicates the algorithmically determined elbow. The minor allele fraction cutoff is indicated within each plot.

**Figure S6.** The number of A>G edits detected at various minor allele fraction cutoffs for the eleven samples with matched DNA data and constrained to regions of high quality using the DNA data. The three SNV calling methods are indicated above the plot and the alignment methods are indicated by the color of the sample. The median is the solid line, the samples with matched exome data are dotted and with matched WGS are solid.

**Figure S7.** Heatmaps of the the average TPR (first column) and percent of the true positives detected in each cell (second column) across the cells from all nine samples after applying increasing coverage cutoffs (y-axis) and average minor allele fraction cutoffs across the cells from

each sample (x-axis) for alignments with scSNV and SNV calls using samtools/bcftools (A), STARSolo with scSNV Pileup (B), and STAR Solo with samtools/bcftools (C).

**Figure S8.** Assessing the effect of saturation on SNV coverage overinflation when using tag counts rather than collapsed molecule counts. For demonstration purposes we used SNVs called with scSNV Pileup for each of the comparisons. A) The average log<sub>2</sub> fold change in STAR Solo tags versus scSNV collapsed molecule counts for true positive SNVs detected in each of the nine samples with matched WGS data. The error bars indicate the standard deviation for each sample. B-D) Examples of the STAR Solo tag coverage versus scSNV collapsed molecule coverage for samples with various saturation percentages as indicated above the plots.

**Supplemental Table S1.** Samples processed in this study

**Supplemental Table S2.** Sample SNV summary data for accuracy calculations

**Supplemental Table S3.** Summary of accuracy rates for individual cells

# Figure S1

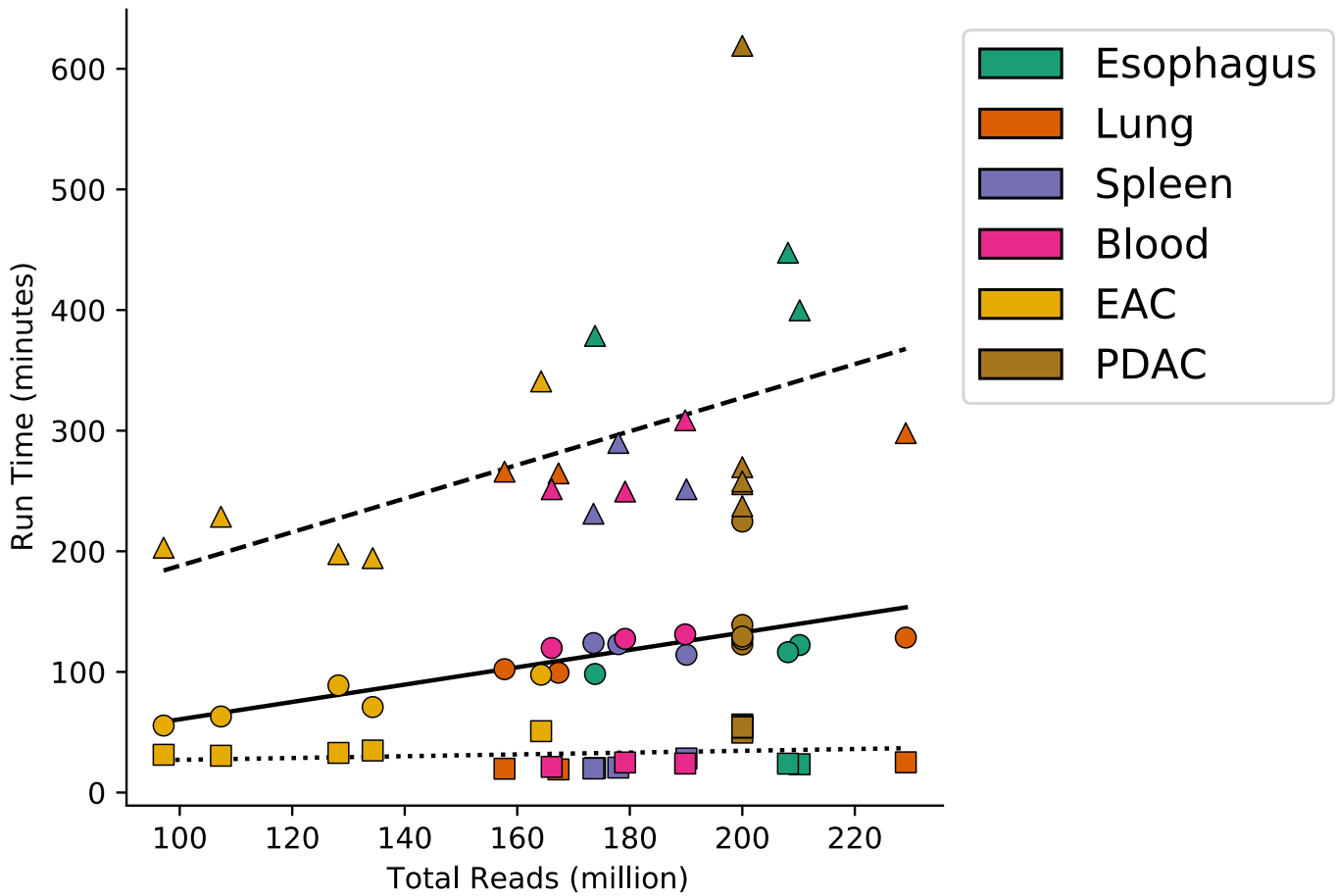


# Figure S2

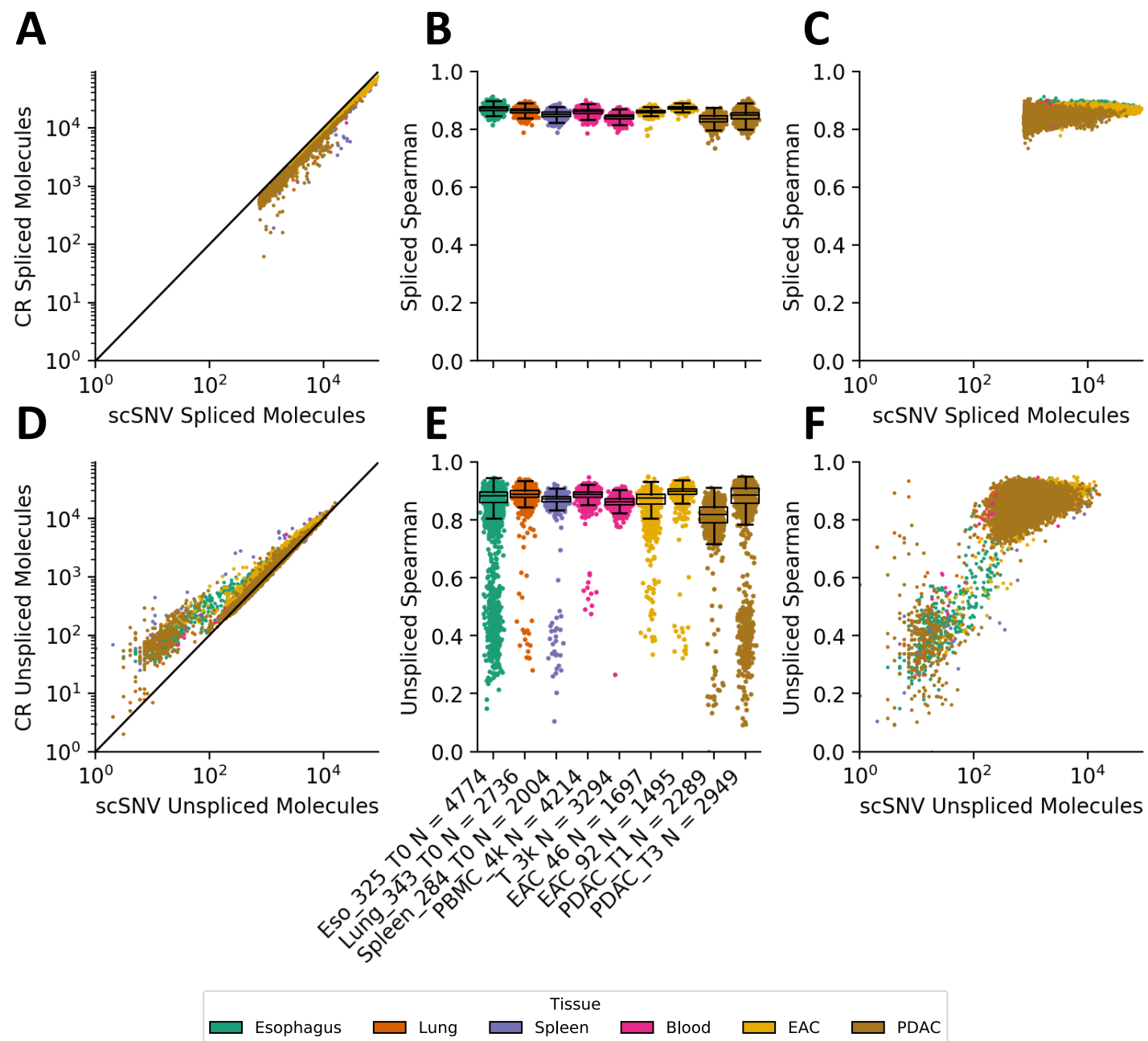
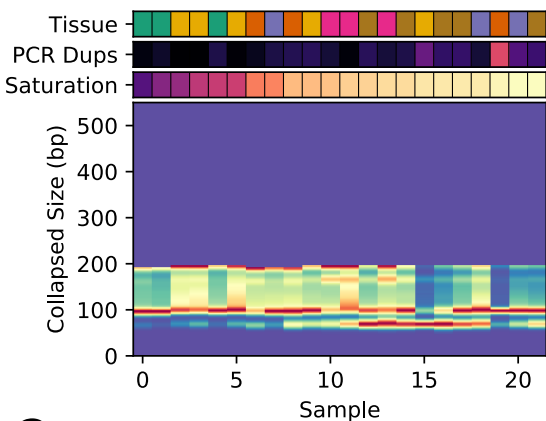
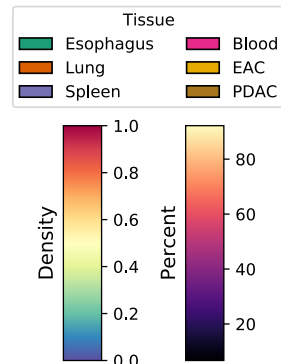
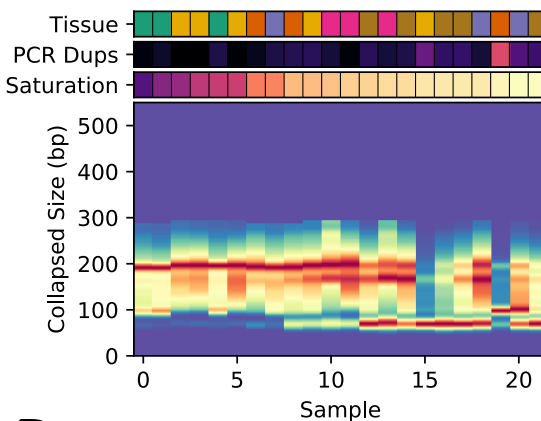


# Figure S3

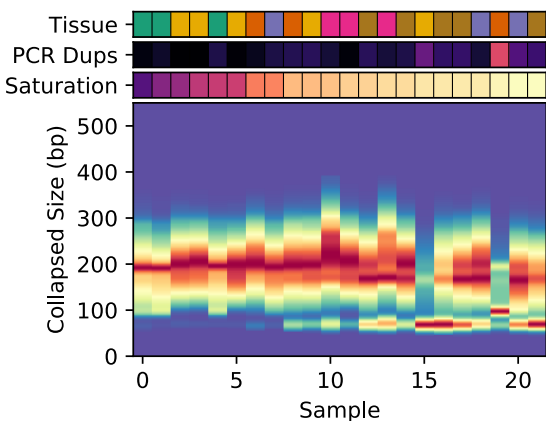
## A



## B



## C



## D

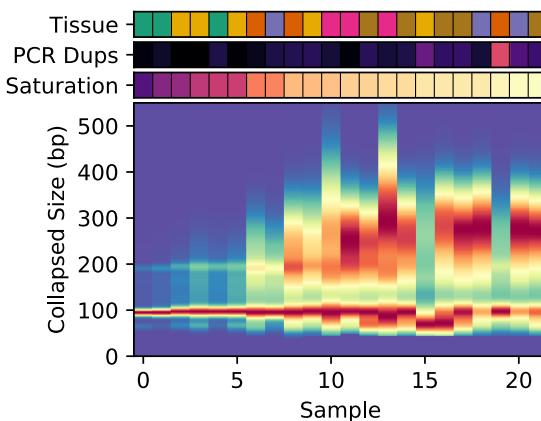


# Figure S4

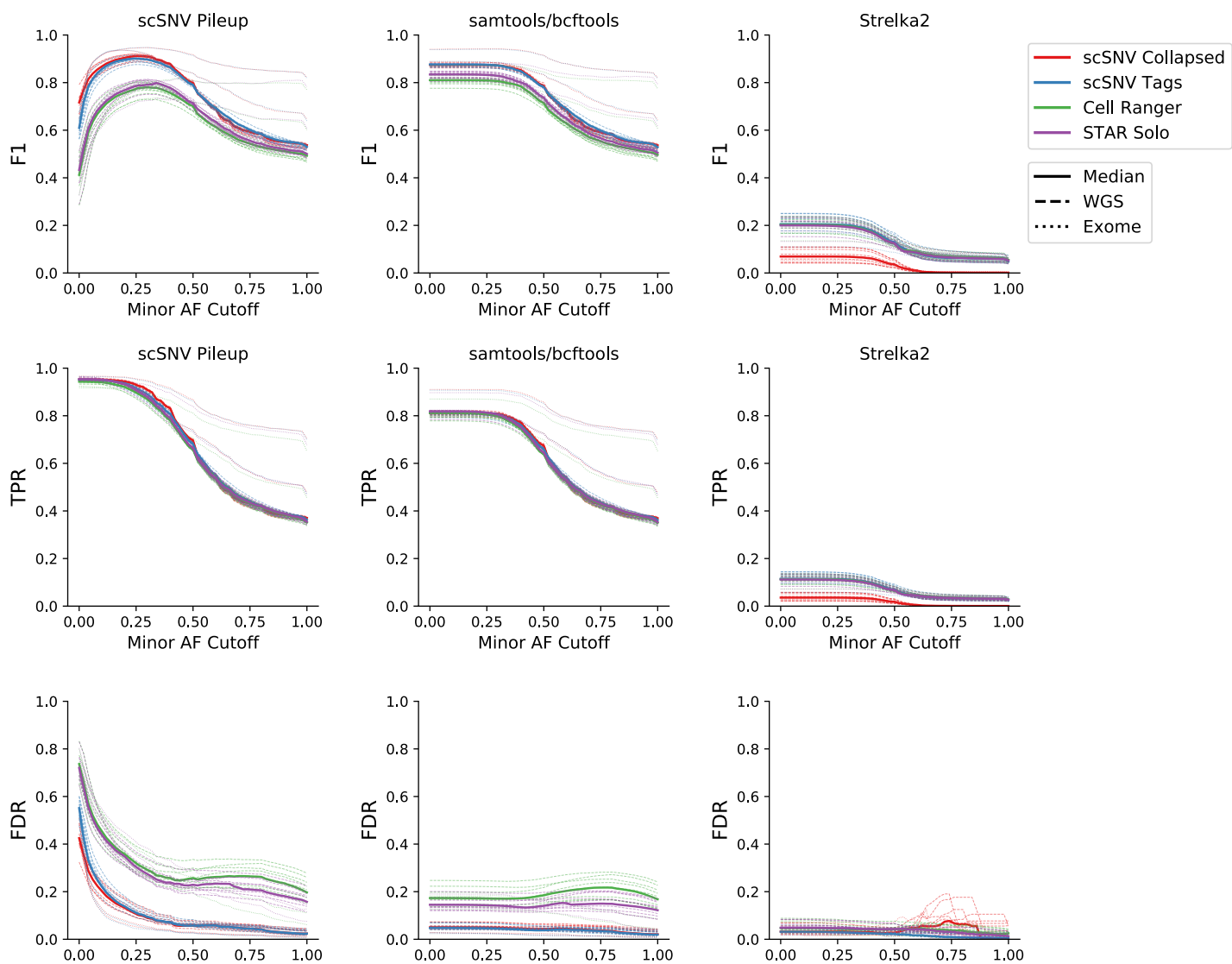


# Figure S5

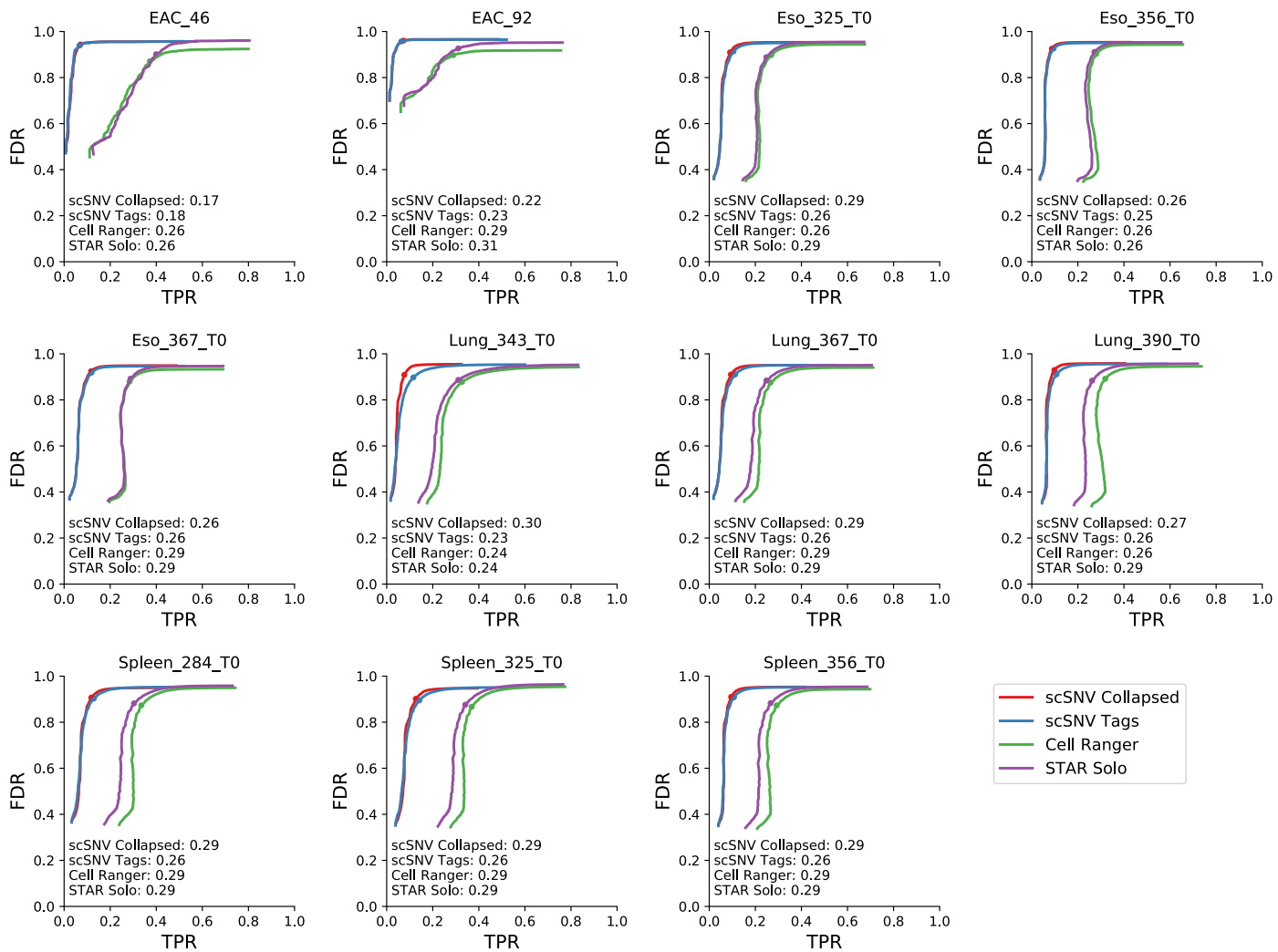




# Figure S6

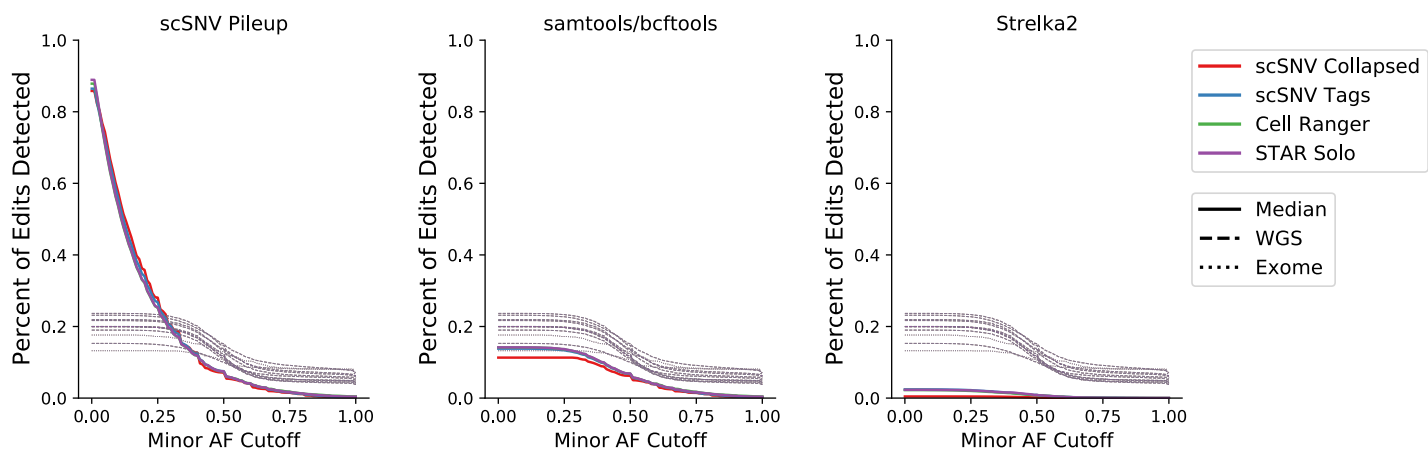


# Figure S7

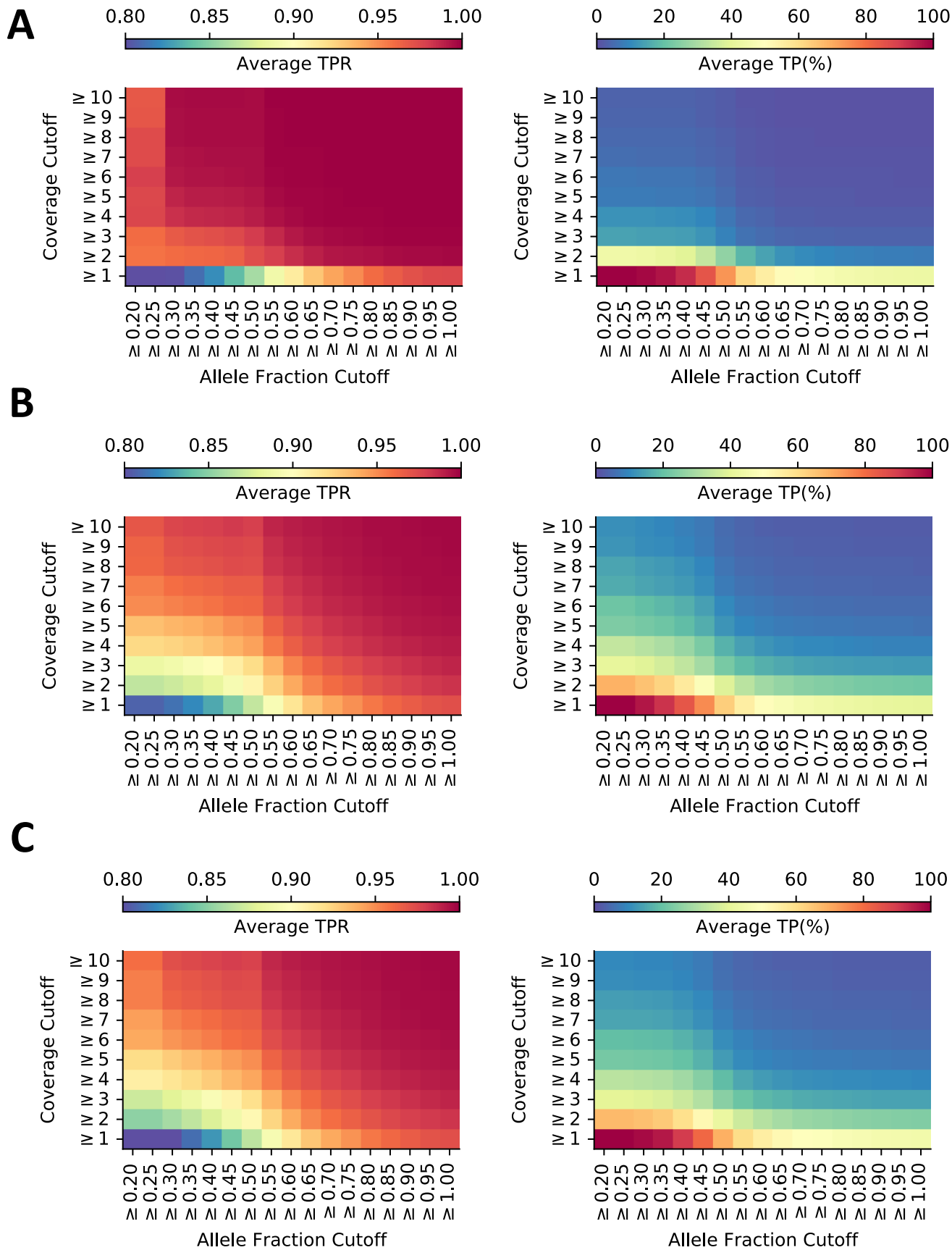
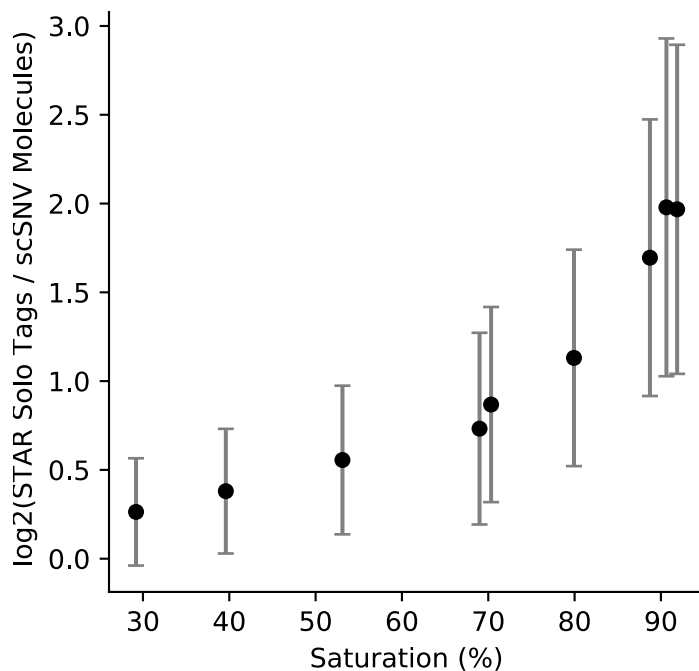
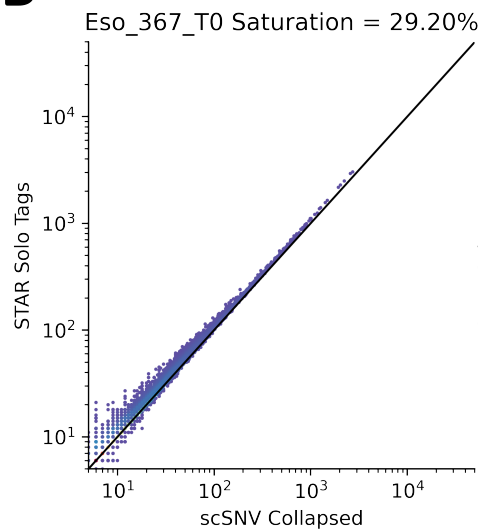


# Figure S8

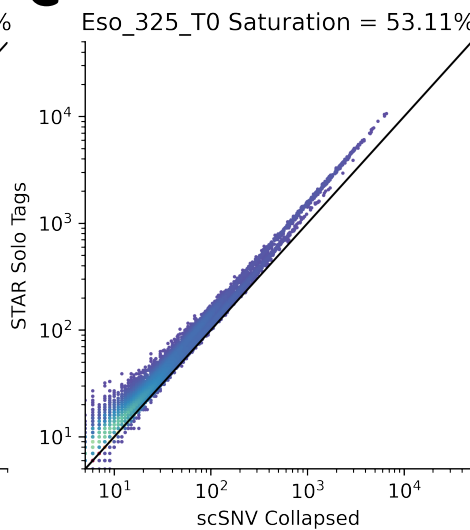
## A



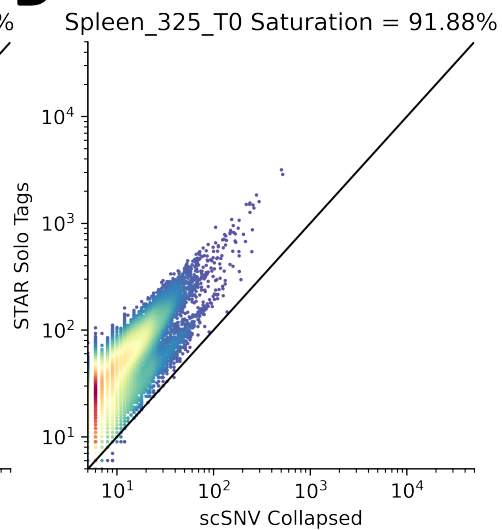
## B



## C



## D



Density

